doi:10.1093/brain/awr160 Brain 2011: 134; 2548–2564 | 2548

BRAIN
A JOURNAL OF NEUROLOGY

A comparative clinical, pathological, biochemical and genetic study of fused in sarcoma proteinopathies

Tammaryn Lashley,[1] Jonathan D. Rohrer,[2,*] Rina Bandopadhyay,[3,*] Charles Fry,[1] Zeshan Ahmed,[1] Adrian M. Isaacs,[4] Jack H. Brelstaff,[1,3] Barbara Borroni,[2] Jason D. Warren,[2] Claire Troakes,[5] Andrew King,[6] Safa Al-Saraj,[6] Jia Newcombe,[7] Niall Quinn,[8] Karen Ostergaard,[9] Henrik Daa Schrøder,[9] Marie Bojsen-Møller,[10] Hans Braendgaard,[10] Nick C. Fox,[2] Martin N. Rossor,[2] Andrew J. Lees,[1,3] Janice L. Holton[1] and Tamas Revesz[1]

1 Queen Square Brain Bank for Neurological Disorders, UCL Institute of Neurology, 1 Wakefield Street, London WC1N 1PJ, UK
2 Dementia Research Centre, UCL Institute of Neurology, Queen Square, London WC1N 3BG, UK
3 Reta Lila Weston Institute, UCL Institute of Neurology, 1 Wakefield Street, London WC1N 1PJ, UK
4 Department of Neurodegenerative Disease, UCL Institute of Neurology, University College London, London WC1N 3BG, UK
5 MRC Neurodegenerative Brain Bank, Institute of Psychiatry, King's College London, London SE5 8AF, UK
6 Department of Clinical Neuropathology, King's College Hospital, London SE5 8AF, UK
7 NeuroResource, UCL Institute of Neurology, 1 Wakefield Street, London WC1N 1PJ, UK
8 The National Hospital for Neurology and Neurosurgery, Queen Square, London WC1N 3BG, UK
9 Department of Neurology, Odense University Hospital, 5000 Odense C, Denmark
10 Arhus Kommunehospital, Neuropathology Department, 8000 Arhus C, Denmark

*These authors contributed equally to this work.

Correspondence to: Prof. Tamas Revesz,
Queen Square Brain Bank,
Institute of Neurology,
Queen Square,
London WC1N 3BG, UK
E-mail: t.revesz@ion.ucl.ac.uk

Neuronal intermediate filament inclusion disease and atypical frontotemporal lobar degeneration are rare diseases characterized by ubiquitin-positive inclusions lacking transactive response DNA-binding protein-43 and tau. Recently, mutations in the fused in sarcoma gene have been shown to cause familial amyotrophic lateral sclerosis and fused in sarcoma-positive neuronal inclusions have subsequently been demonstrated in neuronal intermediate filament inclusion disease and atypical frontotemporal lobar degeneration with ubiquitinated inclusions. Here we provide clinical, imaging, morphological findings, as well as genetic and biochemical data in 14 fused in sarcoma proteinopathy cases. In this cohort, the age of onset was variable but included cases of young-onset disease. Patients with atypical frontotemporal lobar degeneration with ubiquitinated inclusions all presented with behavioural variant frontotemporal dementia, while the clinical presentation in neuronal intermediate filament inclusion disease was more heterogeneous, including cases with motor neuron disease and extrapyramidal syndromes. Neuroimaging revealed atrophy of the frontal and anterior temporal lobes as well as the caudate in the cases with atypical frontotemporal lobar degeneration with ubiquitinated inclusions, but was more heterogeneous in the cases with neuronal intermediate filament inclusion disease, often being normal to visual inspection early on in the disease. The distribution and severity of fused in sarcoma-positive neuronal cytoplasmic inclusions, neuronal intranuclear inclusions and neurites were recorded and fused in sarcoma was biochemically analysed in both subgroups. Fused in sarcoma-positive neuronal cytoplasmic

Received March 5, 2011. Revised May 16, 2011. Accepted May 16, 2011. Advance Access publication July 12, 2011

and intranuclear inclusions were found in the hippocampal granule cell layer in variable numbers. Cortical fused in sarcoma-positive neuronal cytoplasmic inclusions were often 'Pick body-like' in neuronal intermediate filament inclusion disease, and annular and crescent-shaped inclusions were seen in both conditions. Motor neurons contained variable numbers of compact, granular or skein-like cytoplasmic inclusions in all fused in sarcoma-positive cases in which brainstem and spinal cord motor neurons were available for study (five and four cases, respectively). No fused in sarcoma mutations were found in any cases. Biochemically, two major fused in sarcoma species were found and shown to be more insoluble in the atypical frontotemporal lobar degeneration with ubiquitinated inclusions subgroup compared with neuronal intermediate filament inclusion disease. There is considerable overlap and also significant differences in fused in sarcoma-positive pathology between the two subgroups, suggesting they may represent a spectrum of the same disease. The co-existence of fused in sarcoma-positive inclusions in both motor neurons and extramotor cerebral structures is a characteristic finding in sporadic fused in sarcoma proteinopathies, indicating a multisystem disorder.

Keywords: frontotemporal lobar degeneration; FUS; clinical presentation; neuropathology; biochemistry

Abbreviations: FTLD-U = frontotemporal lobar degeneration with ubiquitinated inclusions; FUS = fused in sarcoma; NIFID = neuronal intermediate filament inclusion disease; SDS = sodium dodecyl sulphate; TDP = transactive response DNA-binding protein

Introduction

Frontotemporal lobar degenerations are a group of neurodegenerative diseases known to have overlapping clinical syndromes, with a number of different underlying pathological phenotypes (Neary *et al.,* 1998). The three best delineated clinical syndromes are behavioural variant frontotemporal dementia, progressive non-fluent aphasia and semantic dementia, although the clinical subtypes do not always predict the underlying degenerative disease.

As a result of recent advances in our understanding of the molecular mechanisms associated with frontotemporal lobar degeneration, this heterogeneous group of diseases are now subdivided on the basis of the presence of abnormal intracellular protein aggregates (Mackenzie *et al.,* 2010). In approximately half of all cases with frontotemporal lobar degeneration, the hyperphosphorylated tau protein forms inclusions in neurons and in some forms also in glia. The majority of the tau-negative cases have neuronal inclusions originally identified by their immunoreactivity for ubiquitin and designated as frontotemporal lobar degeneration with ubiquitinated inclusions (FTLD-U) (Josephs *et al.,* 2004; Mackenzie *et al.,* 2006). The majority of the FTLD-U cases have been demonstrated to be associated with accumulation of the transactive response DNA-binding protein-43 (TDP-43), known as FTLD-TDP (Neumann *et al.,* 2006). In a smaller group of FTLD-U cases with a distinct clinical and morphological phenotype, the ubiquitin-positive inclusions remained negative for TDP-43 and were designated as atypical FTLD-U (Roeber *et al*., 2008). Neuronal intermediate filament inclusion disease (NIFID) or neurofilament inclusion body disease has been defined as a rare form of frontotemporal lobar degeneration with ubiquitin-positive inclusions, a proportion of which are also immunoreactive for α-internexin and neurofilaments (Josephs *et al*., 2003; Cairns *et al*., 2007).

The fused in sarcoma (FUS) protein is composed of 526 amino acids with a molecular weight of 53 kDa and is encoded by the *FUS* gene located on chromosome 16 (Crozat *et al.,* 1993; Aman *et al.,* 1996; Yang *et al.,* 2010). The C-terminal region of the FUS protein contains multiple domains involved in RNA–protein interactions, while the N-terminus is involved in transcription activation (Prasad *et al.,* 1994). FUS is a ubiquitously expressed protein (Aman *et al.,* 1996) that binds RNA (Crozat *et al.,* 1993) and DNA (Perrotti *et al.,* 1998) and is involved in diverse cellular processes including cell proliferation (Bertrand *et al.,* 1999), DNA repair (Baechtold *et al.,* 1999) and RNA transport between intracellular compartments (Zinszner *et al.,* 1997). The subcellular localization of the FUS protein is cell type dependent, for example FUS is present in proportionally larger amounts in the nucleus than in the cytoplasm of neurons while FUS expression is exclusively nuclear in glia (Andersson *et al.,* 2008). The first association between neurodegeneration and FUS was shown in two studies reporting 14 different mutations in the *FUS* gene in 26 unrelated families with familial amyotrophic lateral sclerosis type 6 (Kwiatkowski *et al.,* 2009; Vance *et al.,* 2009). Pathologically, one study reported an increase in neuronal cytoplasmic FUS immunohistochemistry (Kwiatkowski *et al.,* 2009), while the other reported the presence of FUS immunoreactive dystrophic neurites and neuronal cytoplasmic inclusions (Vance *et al.,* 2009). Following these two studies, FUS was shown to be a component of the ubiquitin-positive neuronal cytoplasmic and intranuclear inclusions in a group of FTLDs designated as FTLD-FUS, which includes atypical FTLD-U, NIFID and basophilic inclusion body disease (Munoz *et al.,* 2009; Neumann *et al.,* 2009*a*, *b*; Urwin *et al*., 2010).

The identification of the FUS protein in neuronal inclusions in atypical FTLD-U, NIFID and basophilic inclusion body disease led us to investigate 14 tau and TDP-43 negative FTLD cases identified in the extensive archives of FTLD cases of Queen Square Brain Bank, University College London Institute of Neurology and the Medical Research Council London Brain Bank for Neurodegenerative Diseases, Institute of Psychiatry. The original neuropathological diagnosis was NIFID and atypical FTLD-U in seven cases each. A detailed comparative clinical and neuropathological study was performed using semi-quantitative assessment of

lesions identified by FUS immunohistochemistry. The electrophoretic migration pattern of the FUS protein was investigated using western blot analysis in the 10 cases for which frozen material was available. This study is the first to investigate the molecular composition of the FUS protein in the NIFID subgroup.

Materials and methods

Cases

Brains were donated to the Queen Square Brain Bank for Neurological Disorders, UCL Institute of Neurology, University College London; the Medical Research Council London Brain Bank for Neurodegenerative Diseases, Institute of Psychiatry, King's College, London, UK; Neuropathology Department, Århus Kommunehospital, Århus, Denmark; and NeuroResource, UCL Institute of Neurology, University College London. Demographic and clinical data were obtained from a retrospective case notes review performed by an experienced cognitive neurologist. All patients had details of a standard clinical history and had undergone both neurological examination and cognitive assessment. Magnetic resonance brain imaging was available in six of the cases with NIFID (all but NIFID2) and four of the cases with atypical FTLD-U (Patients 2, 3, 5 and 6). All cases had previously been diagnosed as NIFID ($n = 7$) or atypical FTLD-U ($n = 7$) characterized by the presence of pathological inclusions immunoreactive for ubiquitin, but negative for both tau and TDP-43, with the NIFID subgroup also containing α-internexin-positive inclusions. Eight cases have been previously reported (see Table 1 for summary and references) and six are presented here for the first time. Two cases are from the same family; Patient aFTLD-U7 was the mother of Patient aFTLD-U3.

Immunohistochemistry

Tissue sections (7-μm thick) from a number of brain and spinal cord regions (Table 4) were used. Commercially available anti-FUS antibodies each recognizing different epitopes of the FUS protein were tested (Table 3). FUS immunohistochemistry required pressure cooker pretreatment in citrate buffer (pH 6.0). Endogenous peroxidase activity was blocked with 0.3% H_2O_2 in methanol and non-specific binding with 10% dried milk solution. Tissue sections were incubated with the primary FUS antibodies overnight at 4°C, followed by biotinylated anti-rabbit immunoglobulin G (1:200, 30 min; Dako) and Avidin–biotin complex (30 min; Dako). Colour was developed with diaminobenzidine/H_2O_2. Antibodies to the following proteins were also used: α-synuclein (Vector, 1:50), tau (AT8 clone; Autogen Bioclear, 1:600), TDP-43 (Abnova, 1:800), CD68 (Dako, 1:150), glial fibrillary acidic protein (Dako, 1:1000), p62 (BD Transduction Labs, 1:200) and ubiquitin (Dako, 1:200). Thioflavine-S staining was carried out as previously described (Holton *et al*., 2001). To test the specificity of FUS antibodies, tissue sections from cases with sporadic motor neuron disease with TDP-43-positive inclusions, Alzheimer's disease, Parkinson's disease, multiple system atrophy, Pick's disease, corticobasal degeneration and progressive supranuclear palsy were also used.

Double-label immunofluorescence

The frontal cortex and hippocampal formation from all cases were stained using an anti-FUS antibody (1-50 aa) in combination with either an anti-p62, anti-α-internexin or anti-ubiquitin antibody. After appropriate pretreatment, tissue sections were incubated with the appropriate primary antibody as described above, followed by the secondary antibodies Alexa Fluor 488 and Alexa Fluor 568 (Invitrogen, 1:300) for 1 h at room temperature and 4′-6-diamidino-2-phenylindol (DAPI) was used for nuclear counterstaining. Sections were viewed with a Leica TCS4D confocal microscope using a 3-channel scan head and argon/krypton laser or a fluorescent microscope (Zeiss Axioskop MC80DX).

Assessment of FUS pathology

The extent and severity of FUS-positive pathology was evaluated using a five-tiered semi-quantitative grading scale in which the pathological

Table 1 Demographic data of patients with FUS-positive inclusions

Case no.	References/case	Age of onset (years)	Age at death (years)	Post-mortem delay (h)	Disease duration (years)	Sex	Genetics
NIFID cases							
1	Rohrer *et al.*, 2010, Case 1	27	NA	NA	NA	F	NA
2	Josephs *et al.*, 2003, Case UK1	41	43	55	2	F	No mutations
3	Josephs *et al.*, 2003, Case D1	43	46	30	3	F	No mutations
4	–	44	46	96	2	M	No mutations
5	–	63	68	2	5	F	No mutations
6	–	69	72	90	3	F	No mutations
7	–	32	35	NA	3	M	NA
aFTLD-U cases							
1	Rohrer *et al.*, 2010, Case 4	40	51	12	11	M	No mutations
2	–	43	53	96	10	F	NA
3*	Rohrer *et al.*, 2010, Case 2	44	51	24	7	M	No mutations
4	Rohrer *et al.*, 2010, Case 5	47	52	72	5	M	No mutations
5	Paviour *et al.*, 2004, Case 2	49	55	3.5	6	F	No mutations
6	Rohrer *et al.*, 2010, Case 3	51	60	48	9	M	No mutations
7*	–	55	58	NA	3	F	NA

* Patient aFTLD-U3 (son) is related to Patient aFTLD-U7 (mother).
aFTLD-U = atypical FTLD-U; NA = not available.

Table 2 Behavioural, cognitive and clinical data of the cases with atypical FTLD-U and NIFID

Case no.	Initial diagnosis	Last diagnosis	Behavioural symptoms				Neurological assessment					Cognitive assessment	Other features
			Disinhibition	Apathy	Obsessive compulsive behaviour	Hyperorality or dietary changes	Dysarthria	Bulbar MND/ALS	Limb MND/ALS	Extrapyramidal syndrome	Eye movement abnormality		
NIFID													
1	Unclear	bvFTD	–	+	–	–	+	–	–	–	–	Later episodic memory impairment, executive dysfunction	Inappropriate laughter, limb apraxia
2	CBS	CBS	–	–	–	–	+	–	–	Left arm rigidity and alien limb	Difficulty initiating saccades	Not known	Inappropriate laughter, limb apraxia
3	bvFTD	bvFTD with CBS-like syndrome	+	+	–	+	+	–	–	Bradykinesia and rigidity	–	Executive dysfunction. Later non-fluent aphasia and mutism	Inappropriate laughter, lower limb spasticity
4	Unclear	MND with PSP-like syndrome	–	–	–	–	+	+	+	Bradykinesia and rigidity in all four limbs	Vertical supranuclear gaze palsy, difficulty initiating saccades	Not known	Orofacial apraxia
5	PNFA	MND	–	–	–	–	+	+	+	–	–	Non-fluent aphasia	Nil
6	Unclear	MND	–	–	–	–	+	+	+	–	–	Executive dysfunction	Ataxia
7	bvFTD	CBS	–	+	–	+	+	–	–	Bradykinesia and right arm rigidity	Vertical supranuclear gaze palsy	Later episodic memory impairment and executive dysfunction	Limb apraxia, right-sided spasticity and weakness
Atypical FTLD-U													
1	bvFTD	bvFTD	+	+	+	+	–	–	–	–	–	Later episodic memory impairment, executive dysfunction	Nil
2	bvFTD	bvFTD	+	Not known	Not known	Not known	–	–	–	–	–	Not known	Nil
3	bvFTD	bvFTD	+	+	+	+	–	–	–	–	–	Later episodic memory impairment	Nil
4	bvFTD	bvFTD	+	+	–	+	–	–	–	–	–	Executive dysfunction	Visual hallucinations, emotional lability
5	bvFTD	PSP	+	–	–	–	+	–	–	Bradykinesia and rigidity in all four limbs, truncal rigidity	Vertical supranuclear gaze palsy	Executive dysfunction	Inappropriate laughter, hypersexual behaviour
6	bvFTD	bvFTD	–	+	–	–	–	–	–	–	–	Executive dysfunction	Nil
7	bvFTD	bvFTD	+	+	Not known	Not known	–	–	–	–	–	Not known	Nil

ALS = amyotrophic lateral sclerosis; bvFTD = behavioural variant frontotemporal dementia; CBS = Corticobasal syndrome; MND = motor neuron disease; PNFA = progressive non-fluent aphasia; PSP = progressive supranuclear palsy.

Table 3 Anti-FUS antibodies used in this study

Company	Product no.	Type	Epitope	Concentration
Novus Biologicals	NB100-565	Rabbit polyclonal	N-terminus (1–50 aa)	1:200
Novus Biologicals	NB100-562	Rabbit polyclonal	C-terminus (500–526 aa)	1:200
Sigma-Aldrich	HPA008784	Rabbit polyclonal	Mid-region (86–213 aa)	1:200

lesions were scored as '0' that described the absence of FUS-positive neuronal cytoplasmic inclusions and neuronal intranuclear inclusions, score '+' corresponded to 1–5 inclusions present in an average of at least five microscopic fields using a ×20 objective, score '++' was given when the number of lesions was 6–10, while score '+++' was given when the number of inclusions was between 11 and 20. Score '++++' corresponded to >20 lesions. The different morphological neuronal cytoplasmic inclusion types were recorded in each region together with the neuronal intranuclear inclusions. The presence of FUS-positive neurites or glial inclusions was also documented.

Assessment of ubiquitin pathology

The hippocampus and parahippocampus of both NIFID and FTLD-FUS cases were stained with anti-ubiquitin antibodies to reveal ubiquitin-positive inclusions. The inclusions of the granule cell layer of the dentate fascia were analysed and classified into two categories based on the intensity of staining: weak-to-moderate and strong staining categories. Up to 100 inclusions were counted and the difference between the number of weak-to-moderate and strongly staining inclusions for each case and disease subtype was compared and subjected to statistical analysis.

Biochemical fractionation and immunoblot analysis

The method for sequential extraction of proteins with increasing insolubility was an adapted and modified procedure as used in Neumann *et al.* (2009*a*). Frozen material was available in five patients with NIFID and five patients with atypical FTLD-U, three normal controls and two cases with FTLD-TDP. Tissue samples from frontal cortex (grey matter) or spinal cord (one case) were homogenized at a ratio of 1:2 (weight/volume) in high-salt buffer (50 mM Tris–HCl, 750 mM NaCl, 10 mM NaF, 5 mM EDTA) containing 1% Triton-X and protease and phosphatase inhibitors (Roche). Tissue homogenate was initially spun at 1000 *g* to remove nuclear and membrane debris. The resulting supernatant was subjected to ultracentrifugation at 120 000 *g* for 30 min at 4°C, following which the supernatant was retained (high-salt fraction). The pellet was subjected to further extractions with radioimmunoprecipitation buffer (50 mM Tris–HCl, 150 mM NaCl, 1% NP-40, 0.5% deoxycholate) containing 2% sodium dodecyl sulphate (SDS) and protease and phosphatase inhibitors as before, which was subjected to ultracentrifugation at 120 000*g* for 30 min at 15°C to avoid SDS precipitation, with the resulting supernatant being termed radioimmunoprecipitation-SDS fraction. The final pellet was resuspended in 8 M urea containing 8% SDS (urea-soluble) fraction.

Protein concentrations from each fraction were determined by the bicinchoninic acid protein assay (Pierce) and 10, 5 and 0.6 µg of protein from high-salt fraction, radioimmunoprecipitation-SDS fraction and urea fractions, respectively, from each case were loaded onto 10% Bis–Tris polyacrylamide gels (Invitrogen) and run at 200 V with MES [2-(*N*-morpholino)ethanesulphonic acid] buffer (Invitrogen) under reducing conditions. Following electrophoresis, the proteins were transferred onto Hybond P membrane (GE Healthcare), blocked with 5% non-fat dried milk in phosphate-buffered saline containing 0.1% Tween and probed overnight with one of three anti-FUS antibodies, one recognizing the N-terminus (NB100-565; 1:4000), the second the C-terminus (NB100-562; 1:4000) while the third full-length FUS (HPA008784; 1:4000). Following washes in phosphate-buffered saline-Tween, blots were developed using horseradish peroxidase-conjugated secondary antibody (Santa Cruz) and visualized by enhanced chemiluminescence (Pierce) and captured onto Kodak, X-Omat (Sigma) membranes. ImageJ software was used for the semi-quantitative analysis of band density.

For the densitometric quantitation, the densities from the soluble fractions of both the 75 and 53 kDa bands were analysed individually and combined, while for the insoluble component we combined the densities from SDS-soluble and urea-soluble fractions. Results have been expressed as a ratio of soluble/insoluble fractions (Fig. 7).

Genetic testing

Genomic DNA was extracted using a standard method using proteinase K for digestion prior to phenol–chloroform extraction (Laird *et al.*, 1991). The concentration and quality of extracted DNA were determined spectrophotometrically using a Nanodrop (Thermo Scientific). For sequencing of *FUS*, the entire open reading frame and exon–intron boundaries were sequenced; conditions are available on request. The sequences were analysed using the SeqScape software version 2.5 (Applied Biosystems).

Statistical analysis

Statistical analysis was performed using Graphpad Prism 5 software (GraphPad Software Inc.). Continuous variables were analysed using either a two-tailed *t*-test or a Mann–Whitney U test as appropriate, while continuous variables between several groups were compared using the Kruskal–Wallis test. The statistical significance level was established at $P \leqslant 0.05$.

Results

Clinical summary

The NIFID group consisted of five females and two males while the atypical FTLD-U group consisted of three females and four males. The mean age of onset was similar in both groups: mean 45.6 (SD 15.3) years old in the NIFID group and 47.0 (SD 5.1) years old in the atypical FTLD-U group. However, the variability of age of onset was greater in the NIFID group with a range of 28–69 years, with a much smaller range of 40–55 years in the atypical FTLD-U group. There was a significant difference between

the disease duration from symptom onset to death between the groups with a shorter, relatively rapid, disease course in the NIFID group: mean 3.0 (SD 1.1) years compared with a longer disease duration in atypical FTLD-U of 7.3 (SD 2.9) years (Students *t*-test; $P = 0.003$).

The most common syndromic diagnosis was the behavioural variant of frontotemporal dementia and all the patients with atypical FTLD-U had initial behavioural features with a combination of disinhibition, apathy, obsessive/compulsive behaviour and change in appetite (usually development of a 'sweet tooth'). Patients later developed cognitive impairment with most prominently executive dysfunction and often episodic memory impairment as well. This group includes four cases previously reported in Rohrer *et al.* (2010) (aFTLD-U1, 3, 4 and 6). However, one patient with atypical FTLD-U (Case 5) developed falls, truncal rigidity, bradykinesia and rigidity in all four limbs as well as a vertical supranuclear gaze palsy consistent with a progressive supranuclear palsy syndrome [and previously reported as progressive supranuclear palsy with FTLD-U pathology, Case 2, in Paviour *et al.* (2004)]. In contrast, the clinical features of the NIFID cases were more heterogeneous, differing both within group and from the atypical FTLD-U group. Most strikingly, the diagnosis in the NIFID cases was often felt to be unclear initially and not fitting one particular clinical syndrome (all patients attended a specialist tertiary referral centre and were seen by experienced cognitive neurologists). In the youngest patient with NIFID [NIFID1, reported as Case FUS3 in Rohrer *et al.* (2010)], who had behavioural features consistent with the behavioural variant of frontotemporal dementia as well as inappropriate laughter, dysarthria and limb apraxia, this uncertainty led to a brain biopsy being performed. The clinical syndrome of Patient NIFID2 was felt to most closely fit a corticobasal syndrome because of the asymmetrical extrapyramidal syndrome with limb apraxia and alien limb as well as difficulty initiating saccadic eye movements but it was felt to be unusual for corticobasal syndrome because of the rapidity of progression of the disease. The case is reported in more detail as Case UK1 in Josephs *et al.* (2003). Patient NIFID3 [previously reported as Case D1 in Josephs *et al.* (2003)] initially had features consistent with behavioural variant frontotemporal dementia, but later developed parkinsonian and pyramidal features as well as cognitive impairment, leading to an additional diagnosis of a corticobasal syndrome-like syndrome. Patient NIFID7 was also felt to fit most closely to the diagnosis of corticobasal syndrome, and also developed severe dysarthria and a vertical supranuclear gaze palsy. Patients NIFID4, NIFID5 and NIFID6 all eventually had features of motor neuron disease but the initial clinical features differed between the patients and were often non-specific although with relatively intact cognition. Patient NIFID4 presented with right arm weakness, dysarthria and dysphagia. On examination, he was found to have bradykinesia and rigidity in all four limbs without any tremor as well as brisk deep tendon reflexes and a brisk jaw jerk. He developed a vertical supranuclear gaze palsy as well as difficulty initiating saccades. He also had an orofacial apraxia and became anarthric. Two years into the illness, he had an electromyogram showing denervation suggestive of motor neuron disease. Patient NIFID5 presented with progressive impairment of speech production that was slow and monotonous with articulatory difficulties and evidence of phonological errors, although with relatively intact naming. Within the next year, she developed dysphagia and a mixed spastic and flaccid dysarthria. On examination, there was wasting and fasciculations of the tongue and wasting of the left deltoid muscle with brisk deep tendon reflexes and jaw jerk. Electromyography demonstrated chronic partial denervation in all four limbs suggestive of motor neuron disease. The patient became anarthric and writing demonstrated agrammatism and phonological errors. Cognition was otherwise relatively intact in non-linguistic domains, and there were no changes in behaviour or personality. Patient NIFID6 presented with a 12-month history of progressive dysarthria and unsteadiness. She had suffered several falls and required a stick to walk. Neurological examination revealed perioral dyskinesiae, spastic dysarthria with a brisk jaw jerk, hypometric saccades, mild bilateral limb ataxia, retained tendon reflexes and flexor plantar responses, a normal sensory examination and gait ataxia. There was executive dysfunction but otherwise relatively intact cognition. She was reassessed 6 months after her initial presentation: wasting and fasciculations of the tongue and deltoid were noted although an electromyogram was not performed as she was anticoagulated. A clinical diagnosis of motor neuron disease was made at this time.

In the atypical FTLD-U cases, all three patients with imaging had atrophy of the frontal lobe (particularly orbitofrontal cortex), anterior temporal lobe and caudate. Atrophy was asymmetrical with either right- or left-sided predominant atrophy (Fig. 1). As with the clinical features of the group of patients with NIFID, the imaging findings were variable: Patients NIFID 4, 5, 6 and 7 did not have cortical or brainstem atrophy when imaged at the first assessment. Similar to the atypical FTLD-U cases, Patient NIFID1 showed asymmetrical frontotemporal atrophy although to a lesser extent than the atypical FTLD-U cases (Fig. 1). Patient NIFID3 showed caudate atrophy when initially scanned as well as signal change in the striatum although with only mild cortical atrophy. Although MRI was normal initially in Patient NIFID7, a subsequent fluorodeoxyglucose-PET showed asymmetrical reduced uptake in the frontal lobe, worse in the left hemisphere, and an 18F dihydroxyphenylalanine-PET showed reduced uptake in the putamen bilaterally and the left caudate.

In the subgroup of patients with NIFID, the brain weight ranged from 1030 to 1570 g (mean 1256 g) and 780–1274 g (mean 1027 g) in the a subgroup of patients with atypical FTLD-U ($P = 0.1$). The cortical atrophy involved the frontal and anterior temporal lobes, but the parietal and occipital lobes appeared well preserved in all cases. The atrophy was particularly prominent in Patients aFTLD-U3, 5 and 6, in which the most affected gyri had a 'knife-edge' appearance. While some degree of macroscopic changes, indicative of hippocampal sclerosis, were observed in all the cases with atypical FTLD-U, no such macroscopic abnormality was seen in the cases with NIFID. The caudate nucleus was of normal bulk and appearance in all but two patients with NIFID (Cases 2 and 3), which showed severe atrophy and discolouration of this nucleus. In contrast, the caudate nucleus appeared thinned and discoloured in all cases with atypical FTLD-U. In general, the putamen was preserved apart from Patients aFTLD-U5 and 7, in which both the putamen and pallidum were reduced in size and showed greyish discolouration. Spinal cord was available in four

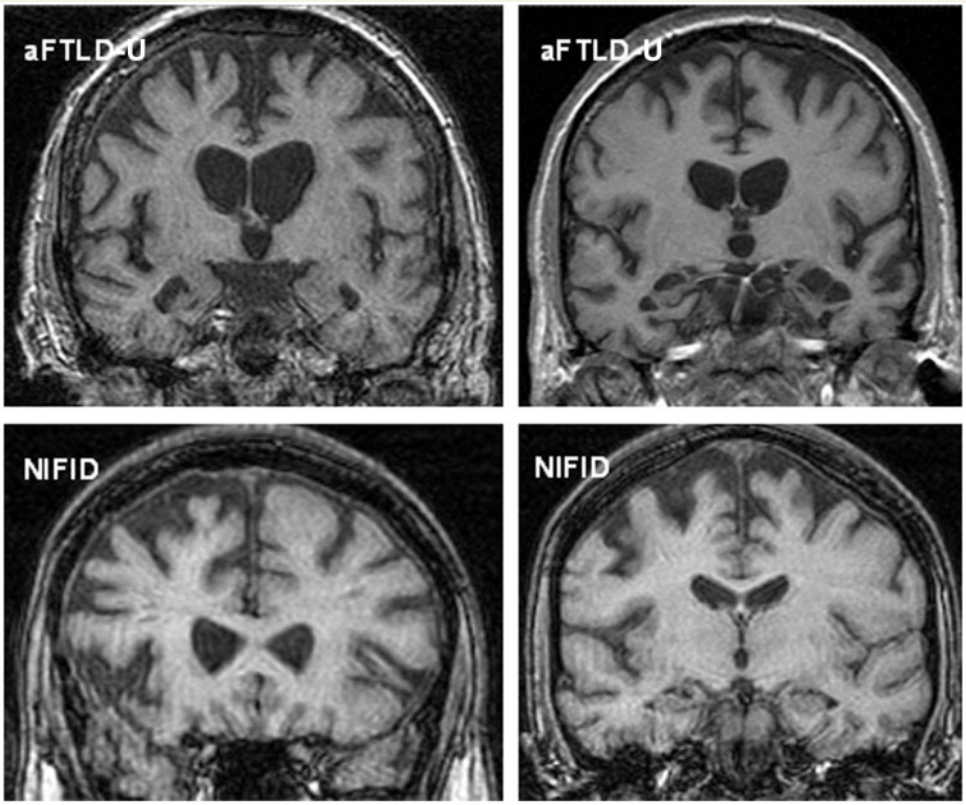

Figure 1 Representative magnetic resonance coronal T_1 images of cases with atypical FTLD-U (*Top left* aFTLD-U6; *Top right* aFTLD-U3) and NIFID (both images from NIFID1). *Top left*: the magnetic resonance image shows asymmetrical right greater than left frontotemporal atrophy; *Top right*: the magnetic resonance image shows asymmetrical left greater than right frontotemporal atrophy. The images on the *bottom* row are from the same patient and show asymmetrical fronto-insular atrophy.

cases with NIFID and three cases with atypical FTLD-U. The cord was described macroscopically as unremarkable in the NIFID cases, but discolouration of the lateral columns was documented in the atypical FTLD-U cases.

Histology

Cerebral cortex

All cases showed superficial spongiosis affecting the frontal and temporal cortices to varying degrees with subpial and white matter gliosis. FUS-positive crescent-shaped neuronal cytoplasmic inclusions were present in all patients, but were more frequent in the cases with NIFID (Fig. 2A) than in the subgroup with atypical FTLD-U (Table 4, Fig. 2F). The superficial cortical layers appeared affected more severely than the deeper cortical laminae in both subgroups. However, the reduced number of inclusions may, at least partially, be the result of the severe cell loss found in the cortex in the subgroup with atypical FTLD-U. In the subgroup with NIFID, further FUS-positive neuronal cytoplasmic inclusion types included large globular or Pick body-like (Table 5) homogenous inclusions and flame-shaped, tangle-like inclusions, which often extended into the apical dendrites of pyramidal neurons. In the subgroup with atypical FTLD-U, bean-like, crescent and annular-shaped FUS-positive inclusions were also present (Table 5; Fig. 2H). An occasional rod-shaped and vermiform neuronal intranuclear inclusion were found in the subgroup with NIFID (Fig. 2D and E), but not in the cortex of the cases with atypical FTLD-U. FUS-positive neurites were found in the white matter of the subgroup with atypical FTLD-U, but not in the subgroup with NIFID. A minority of the neuronal cytoplasmic inclusions were positive for α-internexin in NIFID but they were entirely negative in the cases with atypical FTLD-U (Fig. 4G).

Hippocampal formation

The pathology seen in the hippocampus varied significantly within the two subgroups. Neuronal loss mainly affecting the CA1 hippocampal subregion and subiculum was present in patients NIFID2 and 3, while good preservation of the neuronal population was seen in the hippocampi, subiculum and mediotemporal cortices in the remaining cases with NIFID. The granule cell layer of the dentate fascia and neurons of the subiculum contained large numbers of FUS-positive, bean-shaped or Pick body-like cytoplasmic and intranuclear inclusions in both patients NIFID2 and 3 (Table 5; Fig. 3A and B). Intranuclear inclusions were also frequent in neurons of the granule cell layer of these cases and it was noted that some neurons contained both cytoplasmic and intranuclear inclusions. FUS-positive oligodendroglial coiled body-like inclusions were also seen in the white matter of these two cases. The

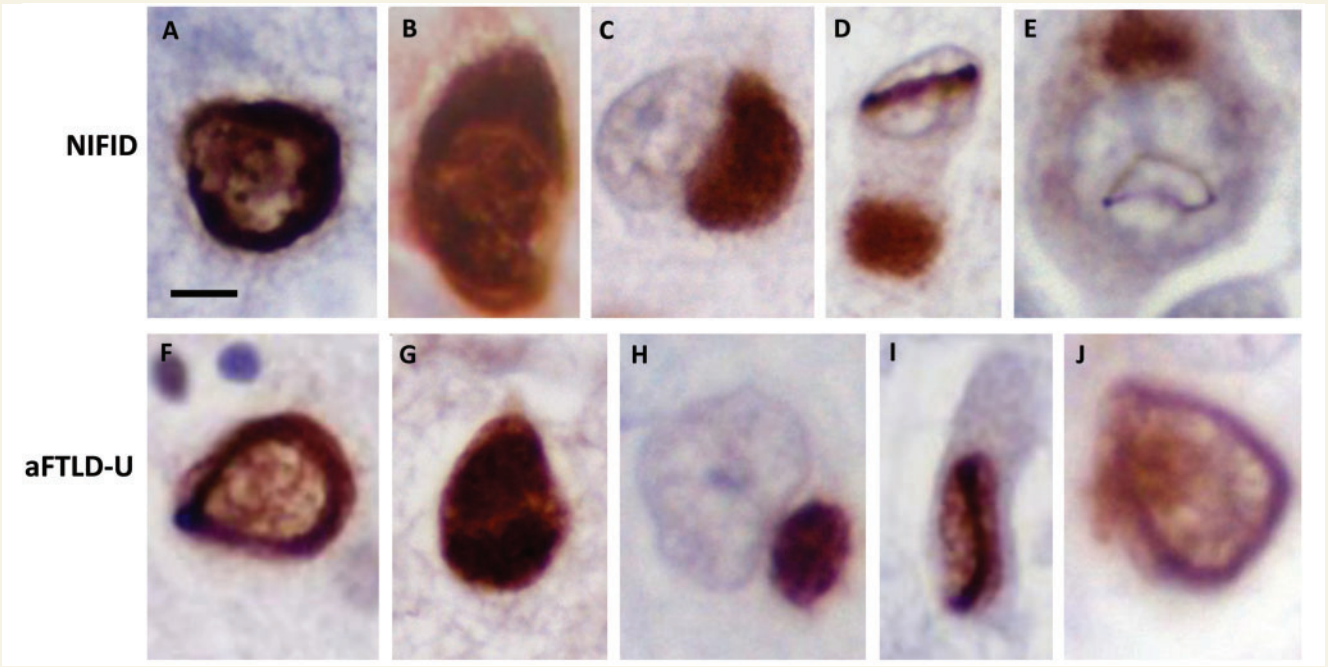

Figure 2 FUS pathology in NIFID and atypical FTLD-U. Different inclusion types were seen in both NIFID and atypical FTLD-U subgroups. Neurons containing crescent/annular-shaped neuronal cytoplasmic inclusions (**A**, **B**, **F** and **G**). The strong nuclear staining is retained in **B** and **G**, while it is decreased in **A** and **F**. Pick body-like inclusions were seen in the NIFID cases (**C**), whereas smaller rounded neuronal 'bean shaped' cytoplasmic inclusions were found in atypical FTLD-U (**H**). Neuronal intranuclear rod shaped (**D** and **I**) and vermiform inclusions (**E** and **J**) were seen in both NIFID and atypical FTLD-U. Scale bar = 5 μm (**A–J**).

Table 4 Distribution of FUS-positive lesions in NIFID and atypical FTLD-U

Anatomical region	NIFID cases							Atypical FTLD-U cases						
	1*	2	3	4	5	6	7	1	2	3	4	5	6	7
Cerebral cortex														
Frontal cortex	+ + + +	+ + + +	+ + +	+ + + +	+ + + +	+ + +	NA	+	+	+	+	+ +	+	+
Temporal cortex	NA	+ +	+ + +	+ +	+ +	+	+ +	+	+	NA	+	+	0	+
Limbic system														
Hippocampus GCL	NA	+ + +	+ + + +	+	+	0	+	+ +	+ + +	+ + +	+ + + +	+	+ +	+
Subiculum	NA	+ + + +	+ + +	+ + +	+	+	NA	0	+	+	+	+	+	+ + +
Entorhinal	NA	+ + +	+ + +	+ +	0	+	NA	+ +	+ +	+ +	+ +	NA	+	+
Fusiform	NA	+ + + +	+ + + +	+	+	+	NA	+	+	+	+ +	NA	+	+
Subcortical nuclei														
Caudate	NA	+ + + +	NA	+ + +	+ + + +	+ + +	NA	+	0	+	+	+ +	NA	NA
Putamen	NA	+ + +	NA	+ + +	+ + + +	+ + +	+ +	+	+	+	+	+ + + +	NA	NA
Globus pallidus	NA	+ + +	NA	+ + +	+	+	NA	NA	0	+	+	+	NA	0
Thalamus	NA	+ +	NA	+ +	+	+ +	NA	NA	NA	NA	NA	NA	0	NA
Brainstem														
Substantia nigra	NA	+ + +	+ + +	+ +	+ +	+	+	NA	NA	+	+	+	+	+
Red nucleus	NA	+ + +	NA	+ +	+ +	+ +	NA	+	NA	0	0	NA	+	0
Locus coeruleus	NA	+ +	+ + + +	+	+	0	NA	NA	0	NA	+	+	+	0
Pontine base	NA	+ +	+ +	+ +	+	+	+	+	+	+	+	+	+	+
12th nerve	NA	+ +	+	+ +	+ + +	+ + +	NA	NA	NA	NA	NA	+ + +	+ +	NA
Spinal cord														
Cervical	NA	NA	NA	+	NA	NA	NA	NA	+ +	NA	NA	+ + +	NA	NA
Thoracic	NA	NA	NA	+	+ +	+	NA	NA	+	NA	NA	NA	NA	NA
Lumbar	NA	NA	+ + +	NA	NA	+ + +	NA	NA	+ +	NA	NA	NA	NA	+ +
Sacral	NA	NA	NA	+	NA	NA	NA	NA	+ +	NA	NA	NA	NA	NA

Score is an aggregate of all FUS-positive lesions, including neuronal cytoplasmic inclusions, neuronal intranuclear inclusions and neurites.
GCL = granule cell layer. Grading: 0 = absent; + = mild; + + = moderate; + + + = frequent; + + + + = severe; NA = not available.
*Patient NIFID1 was diagnosed with a frontal cortical biopsy.

Table 5 Distribution of FUS-positive lesions in NIFID and atypical FTLD-U

Anatomical region	NIFID cases							Atypical FTLD-U cases						
	1*	2	3	4	5	6	7	1	2	3	4	5	6	7
Cerebral cortex														
Frontal cortex	abpv	abpt	abp	abp	avt	at	NA	abt	abt	ab	abt	ab	ab	ab
Temporal cortex	NA	abp	abp	abp	avt	at	ab	abt	abt	NA	abt	ab	0	ab
Limbic system														
Hippocampus GCL	NA	abpvc	abvpc	ab	a	0	NA	bv	bvc	bvc	bvc	bv	bv	bvc
Subiculum	NA	abp	abp	ab	avt	a	NA	0	bt	bvt	bv	b	bv	bv
Entorhinal	NA	abp	abp	ab	0	a	NA	abv	bt	bvt	bv	NA	bvt	bv
Fusiform	NA	abp	abp	ab	at	at	NA	abv	bt	abvt	abvt	NA	bvt	bv
Subcortical nuclei														
Striatum	NA	ba	NA	abvt	abvt	abt	NA	abt	abvt	abt	abt	abt	NA	NA
Globus pallidus	NA	bt	NA	abv	abv	ab	NA	NA	0	ab	ab	ab	NA	0
Thalamus	NA	ag	NA	abv	abv	ab	NA	NA	NA	NA	NA	NA	0	NA
Brainstem														
Substantia nigra	NA	gl bv	gl	gl	gl t	gl	gl	NA	NA	gl v	gl vt	gl	gl	gl
Red nucleus	NA	b	NA	a	bvt	a	NA	b	NA	0	0	NA	b	0
Locus coeruleus	NA	b	gl	gl	gl	0	NA	NA	0	NA	gl vt	gl	gl	0
Pontine base	NA	b	gl b	gl b	gl bv	gl b	gl b	gl	gl vt	v	gl	gl	gl	gl v
12th nerve	NA	gl s	gl s	gl s	gl svt	gl s	NA	NA	NA	NA	NA	gl s	gl s	NA
Spinal cord														
Cervical	NA	NA	NA	gl sg	NA	NA	NA	NA	gl sg	NA	NA	gl sg	NA	NA
Thoracic	NA	NA	NA	gl s	gl st	gl gs	NA	NA	gl sg	NA	NA	NA	NA	NA
Lumbar	NA	NA	gl sg	NA	NA	gl sg	NA	NA	gl sg	NA	NA	NA	NA	gl sg
Sacral	NA	NA	NA	gl s	NA	na	NA	NA	gl sg	NA	NA	NA	NA	NA

* Patient NIFID1 was diagnosed with a frontal cortical biopsy.
Neuronal cytoplasmic inclusion morphologies: a = annular/crescent; b = bean shaped; g = granular; gl = globular; p = Pick body like; s = skein-like filamentous.
Neuronal intranuclear inclusion morphologies: c = circular; v = vermiform.; *t* = FUS-positive neuropil threads; *t* = FUS-positive neuropil threads; NA = not available; GCL = granule cell layer.

remainder of the cases with NIFID demonstrated an occasional crescent-shaped FUS-positive neuronal cytoplasmic inclusion in the granule cell layer of the dentate fascia (Fig. 3C and D), but unlike Patients NIFID2 and 3, no neuronal intranuclear inclusions were seen in the granule cell layer in these cases.

All cases with atypical FTLD-U showed some degree of hippocampal sclerosis. Profound cell loss with marked astrogliosis was seen in the CA1 hippocampal subregion of Patients aFTLD-U3, 6 and 7, which also extended into the subiculum. FUS immunohistochemistry showed that there were frequent neuronal intranuclear inclusions in the granule cell layer of the dentate fascia, which outnumbered the bean-shaped cytoplasmic inclusions found in the same anatomical region in Patients aFTLD-U2, 3 and 4 (Fig. 3D). It is of note that the remaining cases contained only an occasional neuronal cytoplasmic inclusion in the same anatomical area (Fig. 3A). In the CA1 subregion, which was affected by neuronal loss of different degree in all cases, a proportion of the remaining neurons contained cytoplasmic inclusions, intranuclear inclusions or both. Abnormal neurites were also present in the entorhinal cortex and fusiform gyrus.

Subcortical grey nuclei

Patients NIFID2 and 4 showed moderate gliosis in the caudate and putamen, whereas in the remaining cases with NIFID, the basal ganglia appeared unremarkable. FUS immunohistochemistry revealed frequent bean-shaped or ring-like neuronal cytoplasmic inclusions and abnormal neurites in all cases with NIFID in the caudate nucleus and putamen (Table 5). Neuronal vermiform intranuclear inclusions were occasionally observed in Patients NIFID 4 and 5, but were not observed in the other cases with NIFID. In the subgroup with atypical FTLD-U, severe neuronal loss with astrocytosis was seen in the caudate nucleus, putamen and claustrum. Bean and annular-shaped neuronal cytoplasmic inclusions were found in some of the remaining neurons. FUS-positive neuritic profiles were also a prominent feature in the basal ganglia of the subgroup with atypical FTLD-U.

Brainstem

In Patients NIFID5 and 6, the substantia nigra was well populated with neurons and showed only minimal pigment incontinence with an occasional α-synuclein-positive Lewy body and Lewy neurite. The remaining cases with NIFID showed mild neuronal loss in the substantia nigra with extracellular neuromelanin pigment. Globular FUS-positive neuronal cytoplasmic inclusions were found in all cases in the substantia nigra and their number varied from occasional to frequent (Table 4). Apart from Patient NIFID6, where the locus coeruleus remained unaffected, there was neuronal loss in the locus coeruleus in all the cases and several of the remaining neurons contained cytoplasmic inclusions. The neurons of the pontine base were affected in all cases by occasional globular or

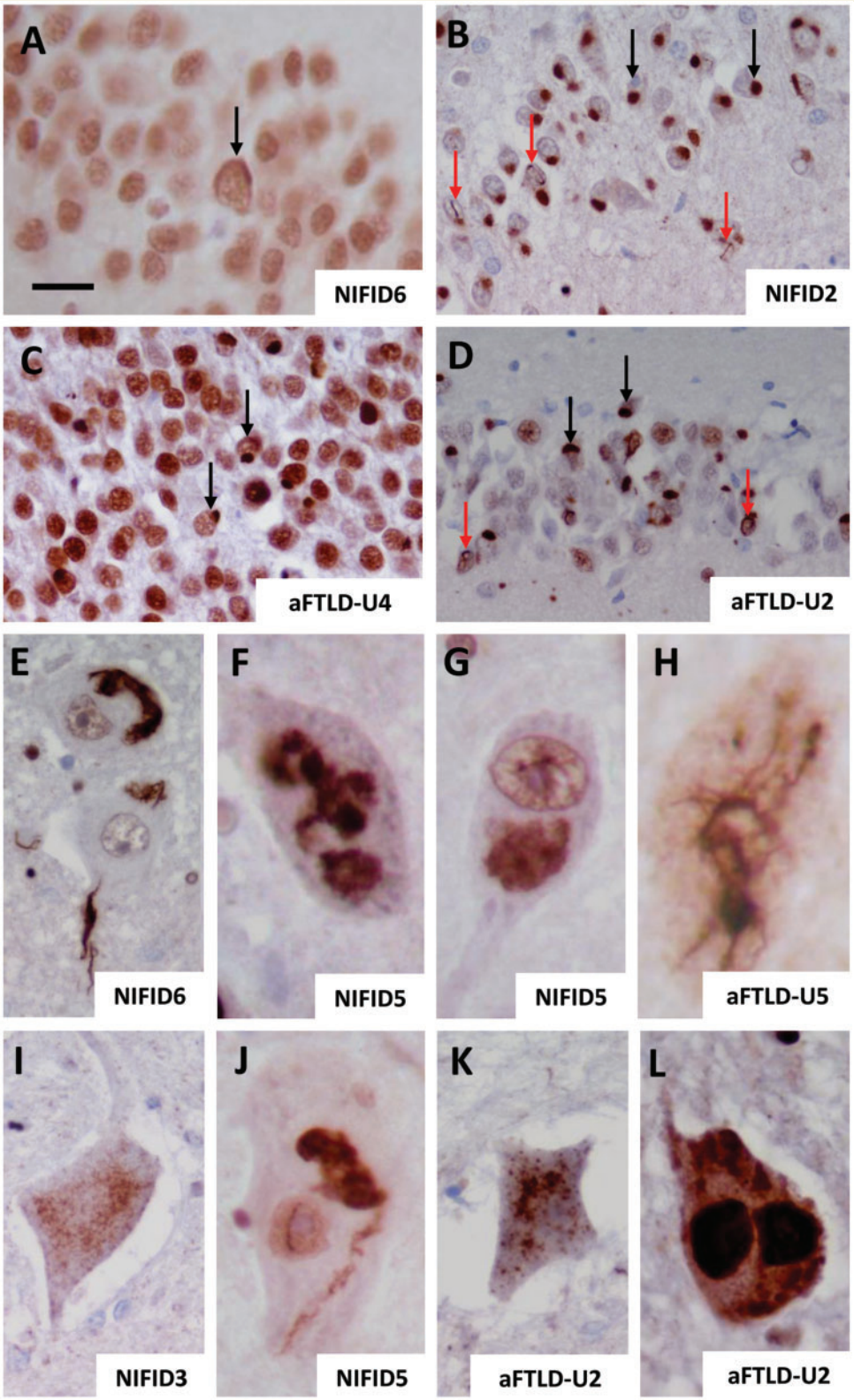

Figure 3 FUS pathology in the hippocampus (**A–D**), 12th cranial nerve nucleus (**E–H**) and spinal cord (**I–L**) in NIFID and atypical FTLD-U. FUS pathology was variable in the hippocampus. Apart from Patient NIFID5 where it was absent, it ranged from mild to severe in both NIFID (**A**: mild, **B**: severe) and atypical FTLD-U (**C**: mild, **D**: severe). Neuronal cytoplasmic inclusions (black arrows) and neuronal intranuclear inclusions (red arrows) were present in the granule cell layer of the dentate fascia in both NIFID and atypical FTLD-U. Different FUS-positive inclusions in motor neurons of the 12th cranial nerve nucleus (**E–H**) and spinal cord (**I–L**), which included filamentous (**E** and **J**), dot-like/granular (**I** and **K**), large globular (**F**, **G** and **L**) and skein-like neuronal cytoplasmic inclusions (**H**) inclusions. Occasional motor neurons also contained intranuclear inclusions (**J**). Scale bar = 20 μm (**A** and **C**); 50 μm (**B** and **D**); and 5 μm (**E–L**).

bean-shaped cytoplasmic inclusions. Although the 12th nerve nucleus showed good preservation of its neuronal population in all cases with NIFID, the majority of the motor neurons contained either compact or filamentous skein-like FUS-positive cytoplasmic inclusions (Fig. 3E–G).

In the subgroup with atypical FTLD-U, the substantia nigra showed severe neuronal loss in all cases with astrocytosis and extraneuronal neuromelanin pigment, together with dense globular FUS-positive neuronal cytoplasmic inclusions. The locus coeruleus also showed cell loss in all cases but this was less severe than that seen in the substantia nigra. An occasional FUS-positive neuronal cytoplasmic inclusion was found in three cases with atypical FTLD-U in the locus coeruleus, whereas two cases remained unaffected (Table 4). The 12th nerve nucleus was available in Patients aFTLD-U5 and 6 where at least half of the motor neurons demonstrated large FUS-positive skein-like filamentous inclusions along with dense globular cytoplasmic inclusions (Fig. 3H).

Cerebellum

Purkinje cell loss and frequent axonal torpedoes were seen in the cerebellar cortex in all cases with NIFID. Purkinje cells contained an occasional FUS-positive intranuclear inclusion in Patient NIFID2. The cerebellar white matter was unremarkable in all cases, but the dentate nucleus showed mild to moderate astrogliosis with occasional globular FUS-positive neuronal cytoplasmic inclusions. Apart from Patients aFTLD-U4 and 7, in which the cerebellum was preserved, the remaining cases with atypical FTLD-U showed loss of Purkinje cells with accompanying Bergmann gliosis and axonal torpedoes. There was mild to moderate astrocytosis in the cerebellar dentate nucleus with occasional dentate nerve cells containing FUS-positive cytoplasmic inclusions.

Spinal cord

Spinal cord was available for assessment from four patients with NIFID. Patient NIFID4 demonstrated pallor of the lateral columns, but the anterior horn cells were preserved in numbers. CD68 immunohistochemistry showed an increase in microglia and macrophages in the lateral columns of the thoracic cord bilaterally in Patient NIFID5, indicating degeneration of the corticospinal tracts. The motor neurons in the thoracic and lumbar cord of Patient NIFID6 and the lumbar cord of Patient NIFID3 showed neuronal cell loss accompanied by increased numbers of microglial and astrocytic cells. A proportion of the motor neurons in all cases with NIFID contained FUS-positive cytoplasmic inclusions, which were either filamentous skein-like, compact, dot-like or had a loose 'cotton wool-like' architecture (Fig. 3I and J). Spinal cord was available for examination in three cases with atypical FTLD-U. The cervical segments showed mild anterior horn cell loss with occasional remaining neurons containing FUS-positive cytoplasmic inclusions. Patient aFTLD-U5 showed degeneration of the crossed and uncrossed corticospinal tracts, while in Patient aFTLD-U7 the spinal cord appeared normal. Skein-like, FUS immunoreactive cytoplasmic inclusions were found in the motor neurons at all levels in all cases (Fig. 3K and L).

Control cases

No labelling of abnormal pathological structures with the anti-FUS antibody was seen in four normal controls and cases with alternative neurodegenerative diseases (sporadic motor neuron disease with TDP-43-positive inclusions, Alzheimer's disease, Parkinson's disease, multiple system atrophy, Pick's disease, corticobasal degeneration and progressive supranuclear palsy).

Thioflavine-S analysis

The inclusions were thioflavine-S-negative in all cases with NIFID and atypical FTLD-U indicating that the FUS protein is not in β-pleated sheet-rich conformation in these diseases.

Double-label immunofluorescence

Double-label immunofluorescence with a combination of anti-FUS and anti-p62 antibodies confirmed that these two antigens co-localize in the neuronal cytoplasmic inclusions (Fig. 4A–F) in both diseases. Double-labelling for FUS and α-internexin (Fig. 4G–I) in the cases with NIFID demonstrated that the co-localization of these two proteins was rather poor within individual inclusions containing both α-internexin and FUS. The majority of the FUS-positive neuronal cytoplasmic and intranuclear inclusions were also labelled with the anti-ubiquitin antibody (Fig. 4N–S), although the ubiquitin staining varied considerably between inclusions in both the NIFID and the atypical FTLD-U cases. Neuronal vermiform intranuclear inclusions were highlighted on thicker sections with FUS immunohistochemistry (Fig. 4J), with an occasional neuron also found to contain a double intranuclear inclusion (Fig. 4K). Several neurons were also noted to contain both cytoplasmic and intranuclear inclusions (Fig. 4L and M).

Ubiquitin and p62 immunohistochemistry

All cases showed positivity to both ubiquitin and p62 to varying degrees, staining neuronal cytoplasmic and intranuclear inclusions in a manner similar to that observed in FUS immunohistochemistry. The intensity of the ubiquitin staining of the inclusions showed considerable variation. The ratio of weakly/moderately and strongly stained inclusions, determined by semi-quantitative analysis in the granule cell layer of the dentate fascia, showed no significant difference in the intensity between the subgroups with NIFID and atypical FTLD-U (*t*-test $P = 0.75$; Fig. 5A and B).

FUS immunoblot analysis

To characterize FUS biochemically, protein was sequentially extracted from flash-frozen frontal cortex from patients with atypical FTLD-U, NIFID, FTLD associated with TDP-43 and controls, using buffers containing increasing detergent strength. FUS immunoreactive bands were consistently detected at ~75 and ~53 kDa in the soluble fraction (high-salt fraction), whereas with some variability in the insoluble fractions (radioimmunoprecipitation-SDS and urea fractions) in all cases using the anti-FUS antibody

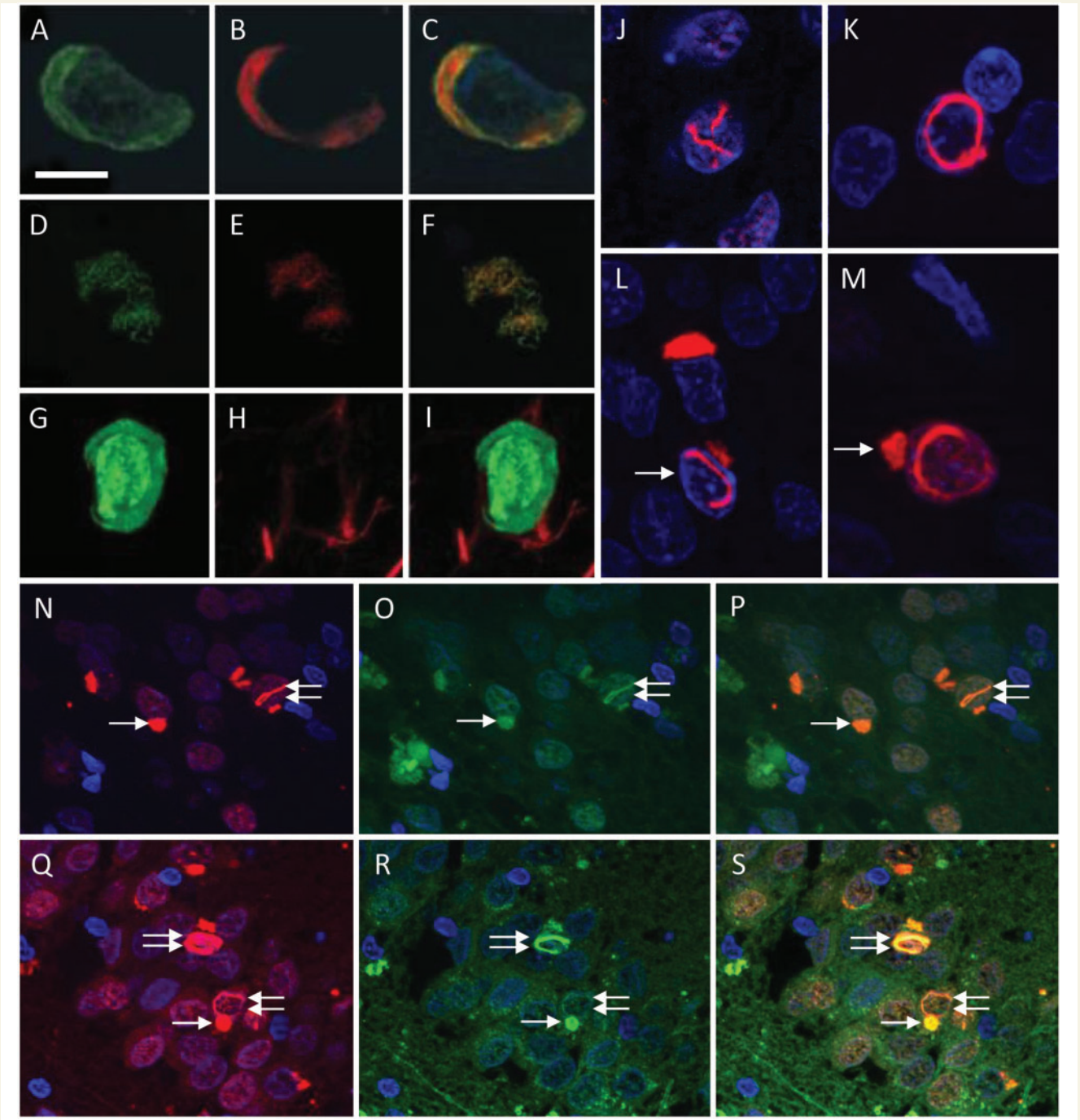

Figure 4 FUS immunofluorescence studies in NIFID and atypical FTLD-U. Double immunofluorescence with FUS (**A** and **D**) and p62 (**B** and **E**; combined images **C** and **F**). Co-localization of FUS and p62 shown in a crescent-shaped inclusion of a frontal cortical neuron (**A–C**) and in a skein-like inclusion of a motor neuron of the 12th nerve nucleus (**D–F**) in NIFID. Double staining with antibodies to FUS and α-internexin (**G–I**) shows absence of α-internexin (**H**) in a FUS-positive cortical neuronal cytoplasmic inclusion (**G**) in NIFID. FUS-positive neuronal intranuclear inclusions demonstrating a number of morphological phenotypes; the image on **J** shows a 'double' intranuclear inclusion while the image on **K** shows a circular neuronal intranuclear inclusion. Some of the neurons on **L** and **M** contained both cytoplasmic and nuclear inclusions (arrows) [(**J–M**) Granule cells of the dentate fascia, Case NIFID6]. Strong colocalization of FUS (**N** and **Q**) and ubiquitin staining (**O** and **R**; combined images **P** and **S**) in both neuronal cytoplasmic (arrow) and neuronal intranuclear inclusions (double arrow) is demonstrated in granule cells of the dentate fascia in NIFID2 (**N–P**) and in Patient aFTLD-U4 (**Q–S**). Scale bar = 10 μm (**A–C** and **G–I**); 20 μm (**J–M**); and 50 μm (**N–S**).

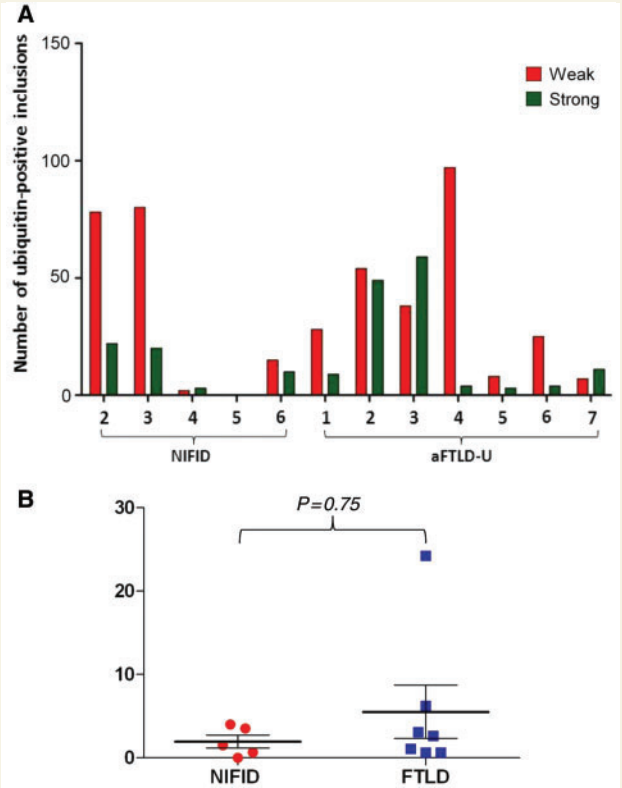

Figure 5 Semi-quantitative analysis of ubiquitin-positive inclusions in NIFID and atypical FTLD-U. In both NIFID and atypical FTLD-U, the intensity of ubiquitin immunoreactivity of the neuronal inclusions varied from weak/moderate to strong, mirroring variation in FUS immunoreactivity. The number of weakly/moderately and strongly stained ubiquitin-positive inclusions were counted in the granule cell layer of the dentate fascia in each case. (**A**) Distribution in the NIFID and atypical FTLD-U cases. (**B**) A ratio of the weakly/moderately and strongly stained inclusions was determined in each case. The mean of the ratios did not differ in the two disease groups (Mann–Whitney U test; $P = 0.75$).

recognizing 1–50 aa (N-terminus). The specificity of the bands was confirmed by (i) an antibody pre-absorption experiment using the relevant synthetic peptide and (ii) omission of the anti-FUS (but not the secondary) antibody (Fig. 6). In these experiments, both the ~75 and the ~53 kDa bands were absent confirming the specificity of the antibody binding and also that the faster migrating 53 kDa band did not represent immunoglobulin recognized by the relevant secondary antibody. Further characterization with two additional antibodies, one recognizing the C-terminus of FUS and the other the full-length protein, also identified the same two bands (data not shown). Further analysis of the immunoblots revealed that in the NIFID cases, the two major bands representing FUS were less abundant in the SDS-soluble fraction than in the soluble (high-salt) fraction. In the urea fraction, while the higher 75 kDa band was abundant, the faster migrating 53 kDa band was absent or very weak in the cases with NIFID (Fig. 6). In contrast, the 75 and 53 kDa bands were represented in all three fractions in atypical FTLD-U. In one case, Patient aFTLD4 (Fig. 6), both bands were stronger in the urea-soluble fraction than those in the SDS-soluble fraction. The 53-kDa bands in both the SDS- and urea-soluble fractions were relatively strong in atypical FTLD-U. The electrophoretic migration pattern of FUS in normal controls (Fig. 6) and FTLD-TDP (data not shown) was similar to that seen in NIFID. Using densitometry for the quantitation of the different bands, a ratio of insoluble (SDS and urea soluble together) to soluble (high-salt soluble) FUS was calculated, which was used as a measure of FUS solubility in each case. This was calculated for the 53 and 75 kDa bands individually and with both bands being pooled together (Fig. 7). Analysing the bands individually, there was a significant overlap between the NIFID, atypical FTLD-U and control groups. However, when the analysis was repeated, combining the bands of the cases with atypical FTLD-U had a statistically significant higher mean ratio of insoluble to soluble FUS (mean = 1.77) than cases with NIFID (mean = 0.64) or controls (mean = 0.96) (Kruskal–Wallis test $P = 0.01$), indicating a decreased solubility of FUS in atypical FTLD-U. However, the difference identified with this approach disappeared when the SDS and urea fractions were analysed independently (SDS/soluble FUS $P = 0.0602$ and urea/soluble FUS $P = 0.0884$).

Genetic analysis of *FUS* gene

Sequencing of all exons of *FUS* did not identify any mutations in the five cases with NIFID and five cases with atypical FTLD-U, where frozen brain tissue was available for DNA extraction and genetic analysis.

Discussion

In this study, we performed a comparative clinicopathological study of seven cases with atypical FTLD-U and seven cases with NIFID and demonstrated a difference between the two subgroups in clinical presentation, pathological features and solubility of FUS. Clinically, all the patients with atypical FTLD-U presented with a behavioural variant of frontotemporal dementia, while the clinical presentation in NIFID was more heterogeneous, including cases with motor neuron disease and extrapyramidal syndromes. Neuroimaging reflected this different clinical pattern with atrophy of the frontal and anterior temporal lobes and caudate in atypical FTLD-U, whereas cases with NIFID were often normal to visual inspection early on in the disease. Our qualitative and semi-quantitative morphological and biochemical analysis of FUS not only showed significant overlap between atypical FTLD-U and NIFID, but also confirmed both morphological and biochemical differences which are characteristic only for either of the two diseases with FUS pathology. We were unable to demonstrate a mutation in the *FUS* gene in 10 cases in which DNA was available for genetic analysis. This is of interest as the cases tested included one of two members of a family (Patients aFTLD-U3 and aFTLD-U7) with confirmed FUS pathology, in whom (Patient aFTLD-U3) no mutation was found in the *MAPT*, *GRN* or *TARDBP* genes either (Rohrer *et al.*, 2009).

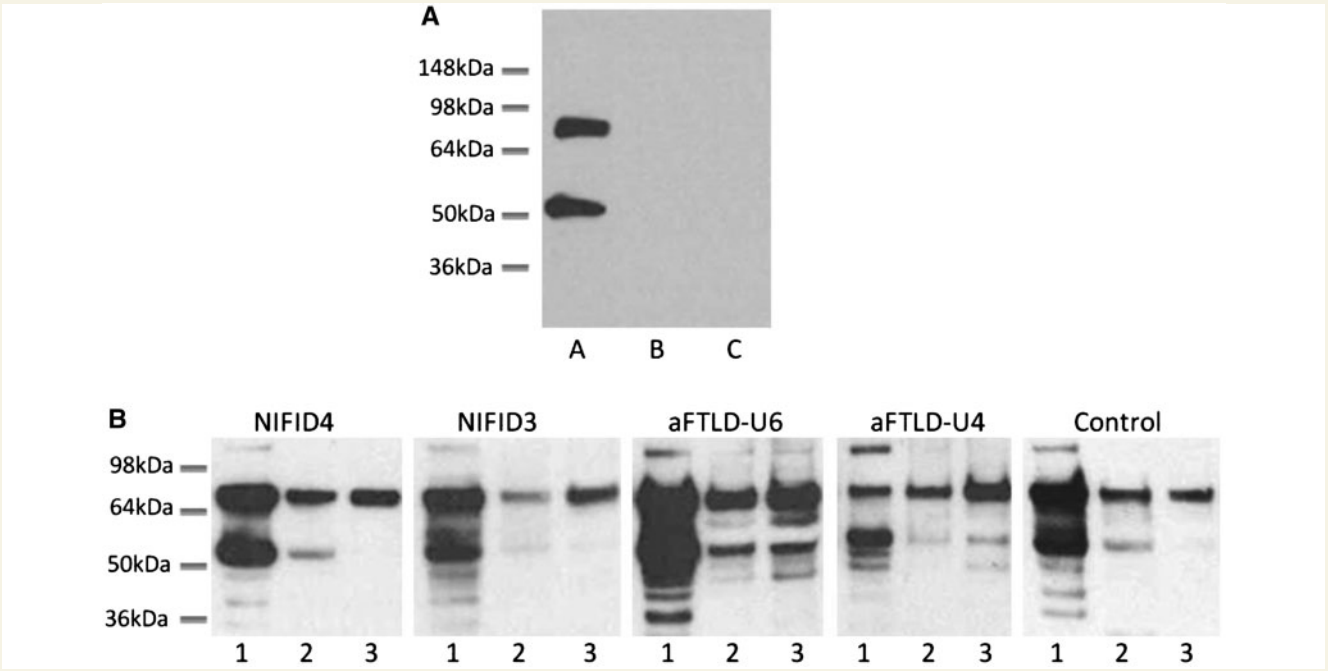

Figure 6 Biochemical analysis of FUS. (**A**) Immunoblotting with a FUS antibody demonstrates two major bands at ~75 and ~53 kDa in NIFID4 (lane A). Control experiments by omitting the primary antibody (lane B) and using a FUS antibody blocked with the corresponding synthetic peptide (lane C) show no visible bands on the western blot. (**B**) Proteins were sequentially extracted from NIFID, atypical FTLD-U and control cases. High salt (lane 1), SDS (lane 2) and urea (lane 3) fractions were separated and immunoblotted with an anti-FUS antibody (NB100-565). All cases showed strong ~75 and ~53 kDa bands in the soluble fraction and a higher band at ~120 kDa was also observed mainly in the soluble fraction. All fractions and all cases contained the higher ~75 kDa band, but the amount of ~53 kDa FUS species varied between cases with a strong band visible in the atypical FTLD-U cases but generally weaker bands in the NIFID and control cases.

Recently, FUS has emerged as a pathological protein in neurodegenerative diseases with striking functional similarities to TDP-43, which together with tau is the most significant pathological protein involved in frontotemporal lobe degeneration and is the most common pathological protein in amyotrophic lateral sclerosis (Neumann *et al.*, 2006). FUS and TDP-43 are DNA/RNA binding proteins involved in gene expression, transcription regulation, RNA splicing, transport and translation (Crozat *et al.*, 1993; Prasad *et al.*, 1994; Aman *et al.*, 1996; Zinszner *et al.*, 1997; Perrotti *et al.*, 1998; Buratti and Baralle, 2008; Yang *et al.*, 2010) continuously shuttling between the nucleus and cytoplasm, although under normal physiological conditions both proteins are predominantly located in the nucleus (Zinszner *et al.*, 1997). The similarities between the two proteins also extend into their roles in disease, as similar to TDP-43, FUS is also implicated in both amyotrophic lateral sclerosis (Neumann *et al.*, 2006; Kwiatkowski *et al.*, 2009; Vance *et al.*, 2009) and FTLD (Neumann *et al.*, 2006, 2009). Mutations of both genes are associated with autosomal-dominant forms of amyotrophic lateral sclerosis with most pathogenic mutations affecting the highly conserved C-termini of the two proteins (Arai *et al.*, 2006; Neumann *et al.*, 2006; Davidson *et al.*, 2007; Kwiatkoski *et al.*, 2009; Vance *et al.*, 2009). One of the significant differences between the TDP-43 and FUS proteinopathies is that under pathological conditions TDP-43 redistributes from the nucleus to the cytoplasm of neurons possessing cytoplasmic inclusions while data from previous (Neumann *et al.*, 2009*a*, *b*) and also by our current investigations indicate that some of the FUS protein is retained within the nucleus of neurons affected by inclusion formation in the FUS proteinopathies.

Although there was overlap between the clinical features of the atypical FTLD-U and NIFID cases, there were a number of key distinctions. Patients with atypical FTLD-U had a mean disease duration of 7 years (similar to other FTLD pathologies) in comparison to the relatively rapid course of the NIFID cases with a mean disease duration of 3 years. Age of onset was often younger than characteristic of FTLD with onset in their 40s or 50s for atypical FTLD-U and although more variable for NIFID, this group included a very young onset case starting in their late 20 s. It has previously been suggested that very early onset frontotemporal dementia (<40 years) is a strong predictor for FUS pathology (Loy *et al.*, 2010). The clinical presentation was relatively homogeneous in the atypical FTLD-U cases, all presenting with behavioural variant of frontotemporal dementia and having asymmetrical orbitofrontal, anterior temporal and caudate atrophy. In contrast, patients with NIFID had a much more heterogeneous clinical presentation with a combination of behavioural, cognitive and motor symptoms. The motor features consisted of either motor neuron disease or an extrapyramidal syndrome (with features of either a corticobasal syndrome or progressive supranuclear palsy syndrome seen)

(Table 2). In comparison to the atypical FTLD-U cases, little cortical or brainstem atrophy was seen early on in many NIFID cases.

The findings of our study using several antibodies to different epitopes of the FUS protein support previous reports showing that FUS is a major pathological protein in neuronal inclusions in both NIFID and atypical FTLD-U (Neumann *et al.,* 2009*b*; Urwin *et al.,* 2010). This also unequivocally redefines NIFID as a FUS proteinopathy, in which only a minority of the inclusions are immunoreactive for α-internexin (Cairns *et al.,* 2004). A number of different neuronal inclusion types were seen in both NIFID and atypical FTLD-U with a significant overlap, and also characteristic differences between the two disease types (Table 5). FUS-positive inclusions were also p62 positive; however, considerable variability was seen in the intensity of staining with ubiquitin immunohistochemistry in both NIFID and atypical FTLD-U. Our semi-quantitative analysis of the intensity of the ubiquitin staining in the granule cell layer of the dentate fascia revealed no difference between NIFID and atypical FTLD-U. Variable labelling of pre-inclusions and larger inclusions with anti-ubiquitin antibodies has also been shown in TDP-43 proteinopathies (Mori *et al.,* 2008; Giordana *et al.,* 2010). According to *in vitro* studies, FUS appears to be one of an unknown number of proteins recognized and degraded by the proteasome without itself undergoing ubiquitination and it is, therefore, possible that the association of FUS with other ubiquitinated molecules is a prerequisite for targeting FUS for proteasomal degradation (Perrotti *et al.*, 1998).

In keeping with data from a recent study, which compared the FUS pathology in atypical FTLD-U, NIFID and basophilic inclusion body disease (Mackenzie *et al.,* 2010), our semi-quantitative assessment of inclusion frequency has confirmed that the FUS pathology was overall considerably more severe in cerebral cortex, medial temporal lobe structures such as subiculum, entorhinal cortex and fusiform gyrus (but not in the granule cell layer of the dentate fascia), subcortical and brainstem nuclei in NIFID than in the same anatomical regions in atypical FTLD-U (Table 4). A greater cell loss in anatomical regions, such as the frontal and temporal cortices and caudate nucleus in the atypical FTLD-U cases may, at least partly, account for the lower numbers of inclusions in these areas, although no such difference in the degree of cell loss could be detected in other subcortical grey and brainstem nuclei, to explain the overall higher number of FUS inclusions in NIFID (Table 4). Hippocampal sclerosis has been described to be a prominent feature of atypical FTLD-U (Roeber *et al.,* 2008; Mackenzie *et al.,* 2010; Urwin *et al.,* 2010) and this was a constant feature of all our cases with atypical FTLD-U and was only present in two of the NIFID cases. With the exception of one case with NIFID the granule cell layer of the dentate fascia was always affected by FUS-positive neuronal inclusions in both disease groups, but it is of note that the number of inclusions tended to be lower or they were even absent in NIFID cases with a clinical presentation indicating motor neuron disease. The overall common and often severe involvement of the neurons of the granule cell layer by FUS-positive inclusions may be due to the reported higher level of cytoplasmic FUS expression within these neurons (Belly *et al.,* 2005), which may render them more vulnerable to inclusion formation (Armstrong *et al.,* 2011). Although only two of our NIFID cases manifested clinically as motor neuron disease, our data indicate that involvement of motor neurons is a general feature of the FUS proteinopathies. Various numbers of FUS-positive neuronal inclusions were seen in motor neurons of the 12th cranial nerve nucleus and of the anterior horns of the spinal cords in NIFID and atypical FTLD-U cases in which the lower brainstem and/or spinal cord were available for neuropathological assessment (five and four cases, respectively). FUS-positive inclusions in motor neurons were morphologically rather diverse and their morphological appearances ranged from granular hazy, cotton wool-like deposits to better defined globular or characteristic skein-like inclusions. The inclusions in motor neurons were also p62 positive, but were only weakly stained with anti-ubiquitin antibody. The finding of constant involvement of motor neurons by FUS-positive inclusions in both NIFID and atypical FTLD-U indicates an increased vulnerability of such neurons to FUS protein aggregation. In post-natal life, a differentially higher level of expression of FUS in motor neurons has been demonstrated in rodents (Huang *et al*., 2010), the relevance of which needs to be confirmed in human disease.

Genetic analysis of exons and splice sites of the *FUS* gene, performed in 10/14 pathologically confirmed cases (five NIFID and five atypical FTLD-U), revealed no mutations. It is of note that DNA extracted from frozen tissue was available for genetic analysis in one (Patient aFTLD-U3) of the two atypical FTLD-U cases that belong to the same family (Patient aFTLD-U7 is the mother of aFTLD-U3) with a history of an autosomal dominant dementing disorder (Rohrer *et al.,* 2010). This observation is in keeping with findings of a recent study reporting two brothers with a dementing illness in one of whom neuropathological examination confirmed FTLD-FUS, but without mutation in the *FUS* gene (Urwin *et al.,* 2010). It remains to be seen whether a mutation in the non-coding region of the *FUS* gene or, analogous with TDP-43 pathology in families with mutation in the *GRN* gene (Baker *et al*., 2006; Cruts *et al.,* 2006), a mutation in another gene functionally linked to FUS is responsible for a familial form of FTLD-FUS.

Using western blots, we were able to perform a comparative biochemical analysis of the FUS protein in NIFID and atypical FTLD-U. Using anti-FUS antibodies recognizing different epitopes, our studies demonstrated two strong bands at 53 and 75 kDa in NIFID, atypical FTLD-U and controls, the specificity of which was confirmed with appropriate experiments (Fig. 6). As the calculated molecular weight of FUS is 53 kDa (Yang *et al.,* 2010), one of the possibilities is that this faster migrating band represents full-length FUS protein without post-translational modifications while the 75-kDa band is a post-translationally modified protein or a protein complex. However, as FUS isolated from cultured cells mainly runs at 75 kDa, it is possible that the 53 kDa band represents a modified protein species. In view of previous findings suggesting the absence of post-translational modifications of FUS (Perrotti *et al.,* 1998) and previous western blot analysis of atypical FTLD-U only demonstrating the slower migrating band (Neumann *et al*., 2009*a*), further studies are required to clarify the composition of both the 53 and 75 kDa FUS protein species. Quantitative analysis of the western blots of our cases demonstrated a significant decrease in solubility of the FUS protein in atypical FTLD-U, but not in NIFID and controls. Our finding of a change in solubility of FUS in atypical FTLD-U is in agreement with a previous report

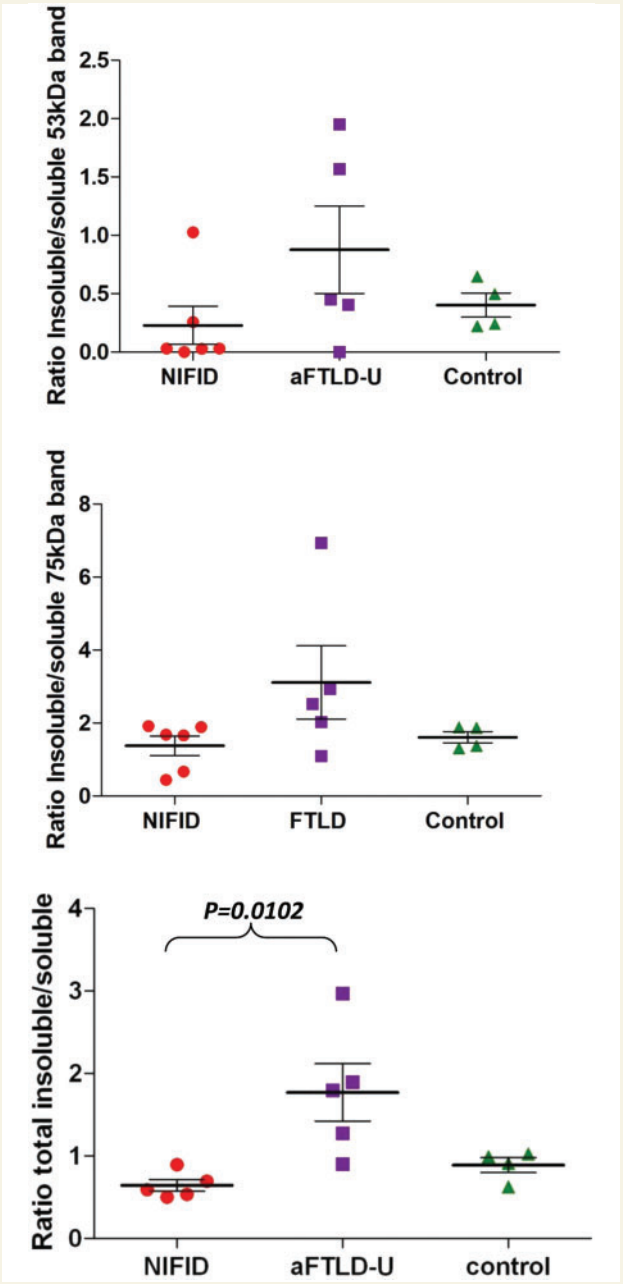

Figure 7 Ratio of insoluble to soluble FUS. The band intensities of FUS in insoluble (SDS and urea soluble) and soluble (PBS soluble) fractions were analysed and a ratio calculated in each case. Bands visible at both ~53 and ~75 kDa were analysed individually and combined to calculate the ratios of total FUS. The ratios are illustrated on the plot with each point representing a case and the solid line representing the mean. Although there is some overlap between the two disease types, the atypical FTLD-U group showed significantly higher ratios compared with both the NIFID and control group when total FUS was analysed (one way Kruskal–Wallis test; $P = 0.01$).

(Neumann *et al*., 2009*a*) but, in addition, our findings also indicate that there may be biochemical differences between the two major subgroups of FUS proteinopathies. To date this shift in solubility of FUS in atypical FTLD-U, shown by Neumann *et al.* (2009) and confirmed by our current study, is the only evidence of disease-associated modification of FUS. As the difference in solubility of FUS between the atypical FTLD-U and NIFID could suggest that the underlying disease mechanisms may also be different in these two forms of FUS proteinopathy, further biochemical investigations are required.

In summary, our study confirms that both NIFID and atypical FTLD-U can be classified under the umbrella term FTLD-FUS. Neuropathologically, they are both characterized by widespread FUS immunoreactive inclusions, affecting several major anatomical areas, including cerebral cortex, subcortical and brainstem nuclei and spinal cord. The distribution and types of FUS inclusions not only show considerable overlap, but also distinct differences in the two diseases. No *FUS* mutations were found in our NIFID and atypical FTLD-U cases, although two of the cases are from the same family raising the possibility of an alternative genetic abnormality. We demonstrated biochemically that FUS is more insoluble in atypical FTLD-U than in NIFID indicating that differences may exist in the underlying mechanisms resulting in aggregation of the FUS protein.

Acknowledgements

The authors would like to thank the patients and their families for their generosity and goodwill, as without their support none of this research would have been possible. This work was undertaken at UCLH/UCL with a proportion of funding from the Department of Health's NIHR Biomedical Research Centres funding scheme. The Queen Square Brain Bank, UCL Institute of Neurology is supported by the Reta Lila Weston Institute of Neurological Studies and the Progressive Supranuclear Palsy (Europe) Association.

Funding

Alzheimer's Research UK to T.R., J.L.H., A.J.L. and M.N.R.; Reta Lila Weston Institute for Neurological Studies to J.L.H.; Wellcome Trust Senior Clinical Fellowship to J.D.W.; J.L.H., T.R. and A.J.L. receive research grants from the Multiple System Atrophy Trust and Parkinson's UK. The Dementia Research Centre is an Alzheimer's Research Trust Coordinating Centre and has also received equipment funded by the Alzheimer's Research UK.

References

Aman P, Panagopoulos I, Lassen C, Fioretos T, Mencinger M, Toresson H, et al. Expression patterns of the human sarcoma-associated genes FUS and EWS and the genomic structure of FUS. Genomics 1996; 37: 1–8.

Andersson MK, Stahlberg A, Arvidsson Y, Olofsson A, Semb H, Stenman G, et al. The multifunctional FUS, EWS and TAF15 proto-oncoproteins show cell type-specific expression patterns and involvement in cell spreading and stress response. BMC Cell Biol 2008; 9: 37.

Arai T, Hasegawa M, Akiyama H, Ikeda K, Nonaka T, Mori H, et al. TDP-43 is a component of ubiquitin-positive tau-negative inclusions in frontotemporal lobar degeneration and amyotrophic lateral sclerosis. Biochem Biophys Res Commun 2006; 351: 602–11.

Armstrong RA, Gearing M, Bigio EH, Cruz-Sanchez FF, Duyckaerts C, Mackenzie IR, et al. The spectrum and severity of FUS-immunoreactive inclusions in the frontal and temporal lobes of ten cases of neuronal intermediate filament inclusion disease. Acta Neuropathol 2011; 121: 219–28.

Baechtold H, Kuroda M, Sok J, Ron D, Lopez BS, Akhmedov AT. Human 75-kDa DNA-pairing protein is identical to the pro-oncoprotein TLS/FUS and is able to promote D-loop formation. J Biol Chem 1999; 274: 34337–42.

Baker M, Mackenzie IR, Pickering-Brown SM, Gass J, Rademakers R, Lindholm C, et al. Mutations in progranulin cause tau-negative frontotemporal dementia linked to chromosome 17. Nature 2006; 442: 916–9.

Belly A, Moreau-Gachelin F, Sadoul R, Goldberg Y. Delocalization of the multifunctional RNA splicing factor TLS/FUS in hippocampal neurones: exclusion from the nucleus and accumulation in dendritic granules and spine heads. Neurosci Lett 2005; 379: 152–7.

Bertrand P, Akhmedov AT, Delacote F, Durrbach A, Lopez BS. Human POMp75 is identified as the pro-oncoprotein TLS/FUS: both POMp75 and POMp100 DNA homologous pairing activities are associated to cell proliferation. Oncogene 1999; 18: 4515–21.

Buratti E, Baralle FE. Multiple roles of TDP-43 in gene expression, splicing regulation, and human disease. Front Biosci 2008; 13: 867–78.

Cairns NJ, Bigio EH, Mackenzie IR, Neumann M, Lee VM, Hatanpaa KJ, et al. Neuropathologic diagnostic and nosologic criteria for frontotemporal lobar degeneration: consensus of the Consortium for Frontotemporal Lobar Degeneration. Acta Neuropathol 2007; 114: 5–22.

Cairns NJ, Zhukareva V, Uryu K, Zhang B, Bigio E, Mackenzie IR, et al. Alpha-internexin is present in the pathological inclusions of neuronal intermediate filament inclusion disease. Am J Pathol 2004; 164: 2153–61.

Crozat A, Aman P, Mandahl N, Ron D. Fusion of CHOP to a novel RNA-binding protein in human myxoid liposarcoma. Nature 1993; 363: 640–4.

Cruts M, Kumar-Singh S, Van BC. Progranulin mutations in ubiquitin-positive frontotemporal dementia linked to chromosome 17q21. Curr Alzheimer Res 2006; 3: 485–91.

Davidson Y, Kelley T, Mackenzie IR, Pickering-Brown S, Du PD, Neary D, et al. Ubiquitinated pathological lesions in frontotemporal lobar degeneration contain the TAR DNA-binding protein, TDP-43. Acta Neuropathol 2007; 113: 521–33.

Giordana MT, Piccinini M, Grifoni S, De MG, Vercellino M, Magistrello M, et al. TDP-43 redistribution is an early event in sporadic amyotrophic lateral sclerosis. Brain Pathol 2010; 20: 351–60.

Holton JL, Ghiso J, Lashley T, Rostagno A, Guerin CJ, Gibb G, et al. Regional distribution of amyloid-Bri deposition and its association with neurofibrillary degeneration in familial British dementia. Am J Pathol 2001; 158: 515–26.

Huang C, Xia PY, Zhou H. Sustained expression of TDP-43 and FUS in motor neurons in rodent's lifetime. Int J Biol Sci 2010; 6: 396–406.

Josephs KA, Holton JL, Rossor MN, Braendgaard H, Ozawa T, Fox NC, et al. Neurofilament inclusion body disease: a new proteinopathy? Brain 2003; 126: 2291–303.

Josephs KA, Holton JL, Rossor MN, Godbolt AK, Ozawa T, Strand K, et al. Frontotemporal lobar degeneration and ubiquitin immunohistochemistry. Neuropathol Appl Neurobiol 2004; 30: 369–73.

Kwiatkowski TJ Jr, Bosco DA, LeClerc AL, Tamrazian E, Vanderburg CR, Russ C, et al. Mutations in the FUS/TLS gene on chromosome 16 cause familial amyotrophic lateral sclerosis. Science 2009; 323: 1205–8.

Laird PW, Zijderveld A, Linders K, Rudnicki MA, Jaenisch R, Berns A, et al. Simplified mammalian DNA isolation procedure. Nucleic Acids Res 1991; 19: 4293.

Loy CT, McCusker E, Kril JJ, Kwok JB, Brooks WS, McCann H, et al. Very early-onset frontotemporal dementia with no family history predicts underlying fused in sarcoma pathology. Brain 2010; 133: e158.

Mackenzie IR, Baborie A, Pickering-Brown S, Du PD, Jaros E, Perry RH, et al. Heterogeneity of ubiquitin pathology in frontotemporal lobar degeneration: classification and relation to clinical phenotype. Acta Neuropathol 2006; 112: 539–49.

Mackenzie IR, Munoz DG, Kusaka H, Yokota O, Ishihara K, Roeber S, et al. Distinct pathological subtypes of FTLD-FUS. Acta Neuropathol 2011; 121: 207–18.

Mori F, Tanji K, Zhang HX, Nishihira Y, Tan CF, Takahashi H, et al. Maturation process of TDP-43-positive neuronal cytoplasmic inclusions in amyotrophic lateral sclerosis with and without dementia. Acta Neuropathol 2008; 116: 193–203.

Munoz DG, Neumann M, Kusaka H, Yokota O, Ishihara K, Terada S, et al. FUS pathology in basophilic inclusion body disease. Acta Neuropathol 2009; 118: 617–27.

Neary D, Snowden JS, Gustafson L, Passant U, Stuss D, Black S, et al. Frontotemporal lobar degeneration: a consensus on clinical diagnostic criteria. Neurology 1998; 51: 1546–54.

Neumann M, Rademakers R, Roeber S, Baker M, Kretzschmar HA, Mackenzie IR, et al. A new subtype of frontotemporal lobar degeneration with FUS pathology. Brain 2009a; 132: 2922–31.

Neumann M, Roeber S, Kretzschmar HA, Rademakers R, Baker M, Mackenzie IR. Abundant FUS-immunoreactive pathology in neuronal intermediate filament inclusion disease. Acta Neuropathol 2009b; 118: 605–16.

Neumann M, Sampathu DM, Kwong LK, Truax AC, Micsenyi MC, Chou TT, et al. Ubiquitinated TDP-43 in frontotemporal lobar degeneration and amyotrophic lateral sclerosis. Science 2006; 314: 130–33.

Paviour DC, Lees AJ, Josephs KA, Ozawa T, Ganguly M, Strand C, et al. Frontotemporal lobar degeneration with ubiquitin-only-immunoreactive neuronal changes: broadening the clinical picture to include progressive supranuclear palsy. Brain 2004; 127 (Pt 11): 2441–51.

Perrotti D, Bonatti S, Trotta R, Martinez R, Skorski T, Salomoni P, et al. TLS/FUS, a pro-oncogene involved in multiple chromosomal translocations, is a novel regulator of BCR/ABL-mediated leukemogenesis. EMBO J 1998; 17: 4442–55.

Prasad DD, Ouchida M, Lee L, Rao VN, Reddy ES. TLS/FUS fusion domain of TLS/FUS-erg chimeric protein resulting from the t(16;21) chromosomal translocation in human myeloid leukemia functions as a transcriptional activation domain. Oncogene 1994; 9: 3717–29.

Roeber S, Mackenzie IR, Kretzschmar HA, Neumann M. TDP-43-negative FTLD-U is a significant new clinico-pathological subtype of FTLD. Acta Neuropathol 2008; 116: 147–57.

Rohrer JD, Guerreiro R, Vandrovcova J, Uphill J, Reiman D, Beck J, et al. The heritability and genetics of frontotemporal lobar degeneration. Neurology 2009; 73: 1451–6.

Rohrer JD, Lashley T, Holton J, Revesz T, Urwin H, Isaacs AM, et al. The clinical and neuroanatomical phenotype of FUS associated frontotemporal lobar degeneration. J Neurol Neurosurg Psychiatry 2010. July 16. [Epub ahead of print] doi:10.1136/jnnp.2010.214437.

Urwin H, Josephs KA, Rohrer JD, Mackenzie IR, Neumann M, Authier A, et al. FUS pathology defines the majority of tau- and TDP-43-negative frontotemporal lobar degeneration. Acta Neuropathol 2010; 120: 33–41.

Vance C, Rogelj B, Hortobagyi T, De Vos KJ, Nishimura AL, Sreedharan J, et al. Mutations in FUS, an RNA processing protein, cause familial amyotrophic lateral sclerosis type 6. Science 2009; 323: 1208–11.

Yang S, Warraich ST, Nicholson GA, Blair IP. Fused in sarcoma/translocated in liposarcoma: a multifunctional DNA/RNA binding protein. Int J Biochem Cell Biol 2010; 42: 1408–11.

Zinszner H, Sok J, Immanuel D, Yin Y, Ron D. TLS (FUS) binds RNA in vivo and engages in nucleo-cytoplasmic shuttling. J Cell Sci 1997; 110 (Pt 15): 1741–50.